NASA Technical Memorandum 102236

Quiet Mode for Nonlinear Rotor Models

R. E. McFarland

April 1990

National Aeronautics and Space Administration

NASA Technical Memorandum 102236

Quiet Mode for Nonlinear Rotor Models

R. E. McFarland, Ames Research Center, Moffett Field, California

April 1990

National Aeronautics and
Space Administration

Ames Research Center
Moffett Field, California 94035-1000

Quiet Mode for Nonlinear Rotor Models

R. E. McFarland

Summary

High frequency harmonics are generated by helicopter rotor systems, and nonlinear, blade-element models of these systems create the same harmonics. In discrete real-time rotorcraft simulation, however, especially for handling qualities research, they are more of a nuisance than a benefit. The cycle times required to adequately represent them are rarely obtainable. The result is that distinct frequencies alias into the pilot and simulator bandwidths, thereby decreasing simulation fidelity.

However, use of an interpolation procedure permits the observation of harmonics at their proper frequency locations, and an accompanying notch filter may then be used to attenuate the harmonics prior to decimation.

Rotorcraft simulations using these techniques are not contaminated with the spurious frequencies that create variable trim points, produce erroneous stability and control derivative data, and obscure time histories.

Discussion

Techniques are used from sample data theory to minimize the adverse effects of aliased harmonics on piloted rotorcraft simulations (real-time versions of Sikorsky GEN/HEL models, refs. 1 and 2). Aliased rotor system harmonics have obscured time histories of simulated vehicle performance for some time (ref. 3). They may even produce fictional pilot tracking tasks.

The subject of aliasing is discussed, and the "aliasing equation" of reference 4 is applied to rotor system harmonics. Appendix A is supplied to familiarize the reader with the mathematical basis for the harmonics.

The UH60 Black Hawk model of reference 2 provides an example for demonstrating both the aliasing phenomenon and the subcycle technique. The relationship of subcycles to a specific blade-level integration algorithm is discussed in appendix B.

A special "Quiet Mode" filter is introduced, which takes advantage of the expanded bandwidth available when the subcycle technique is used. This filter requires a specific discrete implementation.

Numerous dynamic check time histories are presented to support theoretical arguments. For special purpose applications, reconstruction of harmonics is demonstrated.

An important consideration is that the aliasing phenomenon occurs at the communication boundary. This means that small cycle times are not, of themselves, sufficient to eliminate this problem if input-output processes occur at larger cycle times.

Aliasing

In discrete models the total-model cycle time, T, limits the bandwidth, or region of observable frequencies, to the Nyquist frequency, given by (Hz):

$$f_{NYQ} = 1/(2T)$$

This occurs despite the fact that an explicit model expression may purport to create higher frequency content. It also occurs despite the fact that some simulated nonlinear element may produce frequencies beyond the Nyquist limit in the continuum.

Consider, for example, the discrete generation of cosine function data,

$$x_i = \cos(2\pi f_d i T) \qquad (i = 0, 1, 2, ...)$$

where f_d is a "desired frequency," supposedly arbitrary. When f_d is selected to be the Nyquist frequency, the sequence {1,-1,1,-1,...} is created, having the requested frequency content.

However, if f_d is selected to be 50% *greater* than the Nyquist frequency, the sequence that is created {1,0,-1,0,...} only has the frequency of *half* the Nyquist frequency.

Furthermore, if f_d is selected to be twice the Nyquist frequency (*i.e.*, the sample frequency), the sequence that is created {1,1,1,1,...} contains *only a d.c. component.*

This example may be generalized to any frequency generated within a model, whether it be explicitly programmed or a consequence of nonlinear operations.

Frequencies beyond the Nyquist limit appear (will be observed) at different frequencies, *i.e.*, their "destinations." These destinations are always contained within the Nyquist bandwidth. Generally, the resultant frequency "f_r" is the destination of any model frequency "f_d" in accordance with the aliasing equation:

$$f_r = \left| f_d - \left\lfloor \tfrac{1}{2} + f_d T \right\rfloor / T \right|$$

In this equation the lower-bracket expression means the least integer, or "floor", operation. If the desired frequency f_d is less than f_{NYQ} this integer term is zero, and f_r equals f_d.

N/rev Aliasing

In discrete real-time simulation, the value of T must be greater than the actual computer workload. This is required for real-time synchronization of discrete processes with real-world (pilot/simulator) commands. A complex simulation model generally equates to a large cycle time.

The aliasing phenomenon is especially important in rotorcraft models, where the computer workload tends to be high.

Also, blade-element rotorcraft models develop high frequencies. The particular high frequencies of interest to this discussion are those caused by the spectral selection process that occurs in the rotor module during the summation of blade forces and moments. This process is demonstrated in appendix A.

A rotor system produces a fundamental N/rev frequency given by,

$$\Lambda = N\Omega$$

where N is the number of blades, and Ω is the rotor speed, often stated as an RPM (revolutions per minute), but here used in the units of either rad/sec or Hertz.

All harmonics $k\Lambda$ ($k = 1,2,3,...$) of the fundamental frequency are also generated by a nonlinear rotor model, although the magnitudes of these harmonics diminish rapidly with k.

To examine the aliasing phenomenon in a discrete rotorcraft model, consider a rotor system with four blades (N), and a rotor speed of $\Omega = 27$ rad/sec (4.3 Hz). Such a system will produce N/rev harmonic frequencies at 17.2, 34.4, 51.6, ... Hz, which have steady-state magnitudes as well as variable magnitudes excited by transients.

The parameters used in this document are from the real-time GEN/HEL Black Hawk helicopter model. The model is described in ref. 2.

Figure 1 gives the frequency destinations of the first five harmonics produced by this sample rotor system, as functions of the cycle time T. The Nyquist frequency is indicated on these curves by dashed lines.

The magnitude of the kN/rev multiples are known to decrease with increasing k, so that $k > 5$ is not considered in figure 1.

From figure 1(b) a cycle time of about 29 msec causes the 2N/rev signal to alias into the low-frequency bandwidth, whereas from figure 1(c) a cycle time of about 19 msec causes the 3N/rev signal to alias into the low frequency bandwidth. Higher $k\Lambda$ signals alias into the bandwidth with lower cycle times.

Indeed, harmonic multiples may always be found that alias into the low frequency bandwidth. When the original signal has significant magnitude, aliasing produces both spurious low frequency dynamics, and trim point (steady state) errors. These effects are particularly detrimental when $k\Lambda$ frequencies alias into the pilot/vehicle bandwidth, limited by perhaps three Hertz.

Aliasing is easily observed in vehicle acceleration traces. This is demonstrated in figure 2, where the Black Hawk model is in an 80-knot trim condition, using a cycle time of 20 msec. The responses during the first few seconds of operate mode are shown. The linear accelerations have the units of ft/sec^2, and the angular accelerations have the units of rad/sec^2. The vehicle accelerations of figure 2 display the primary characteristics of the "original system," which does not use the noise reduction procedures developed herein.

The aliasing equation reveals that when a realistic cycle time of 20 msec is used, the frequency content of figure 2 consists of the harmonic destinations given in table I:

Table I - Aliased Locations, (20 msec)

N/rev	Origin (Hz)	Destination (Hz)
1	17.189	17.189
2	34.377	15.623
3	51.566	1.566
4	68.755	18.755
5	85.944	14.056

The 3N/rev harmonic predicted to alias to about 1.6 Hz is clearly observed in figure 2. Also, there is considerable activity in the region of 16 Hz, also predicted in table I.

Subcycles

It is useful to define kΛ signals that appear at the wrong frequency as noise. It is also useful to define these signals as noise when their magnitudes and phases are known to be erroneous due to limitations in integration algorithms. These limitations are discussed in *Appendix B.*

The first problem to be addressed, apparent from figures 1 and 2, is to separate signals from noise. This means that the cycle time *within a rotor model* should be small enough that the resultant Nyquist frequency is larger than the first few kΛ multiples, which are known to have significant power (refs. 3 and 4). This problem is compounded when RPM is variable. The maximum RPM is the critical value in the design of an algorithm that will accommodate kΛ multiples. Suppose it is known that a particular rotor speed (during simulation) will never exceed its nominal value Ω_0 (27 rad/sec) by more than 20%. Further suppose that only the first three kΛ must be accommodated within the Nyquist frequency, due to power considerations. Then, for the rotor system with four blades, the Nyquist frequency must satisfy the inequality,

$$f_{NYQ} > (1.2)(3)(4)(27)/2\pi$$

which means that the cycle time must be about 8 msec.

The above restriction, however, cannot always be satisfied. Certain computers cannot perform the requisite workload in 8 msec. Hence, a technique is required that permits higher cycle times by executing just the blade-level equations at smaller cycle times. It is pertinent that these blade-level equations are those which generate the higher harmonics.

A useful technique has been developed that subdivides the rotor model's blade-level equations into subcycles. This technique is called "interpolation" in sample data theory. The subcycles consist of "m" executions at a cycle time of ΔT, where

$$\Delta T = T/m$$

and "m" is given by the greatest integer or "ceiling operator,"

$$m = \lceil 3.6N\Omega_0/\pi \rceil$$

The value for ΔT is thus a fraction of the total-model cycle time T; it assures that the 3Λ frequency remains within the subcycle's Nyquist frequency, despite RPM variations. As shown in figure 3, the technique assures that the subcyclic interval is small enough to accommodate the 3Λ signal.

The subcycle technique requires few changes in the rotor module. The suggested structure is given in figure 4, where "NQ" is the number of subcycles, "NB" is the number of blades, and "NS" is the number of segments per blade. Everything in the subcycle loop is executed every ΔT, and everything outside this loop is executed every T.

For the original cycle time of T = 20 msec, the subcycle technique produces an internal rotor cycle time of ΔT = 6.67 msec (three subcycles). The outputs of the rotor module are then decimated (every third cycle used) when communication is made with the rest of the rotorcraft model. Using this procedure the acceleration histories are modified as shown in figure 5. Most channels produce a decrease in noise level because algebraic loops contained entirely within the rotor model are executed three times as often.

The second problem to be addressed concerns the decimation operation (the inverse operation of interpolation). As shown by the limited noise reduction of figure 5, great success cannot be expected in computing a model subsystem using a high Nyquist frequency if it is then decimated when communicating with the rest of the rotorcraft model. The frequency content would then be aliased back to where it would have originally occurred by using the lower Nyquist frequency. A certain amount of accuracy improvement may be obtained by this procedure when algebraic loops exist within the subsystem, but high frequencies will still alias into the low frequency region at the communication boundary.

For this reason, deliberate signal attenuation must occur *during* the subcycle loop so that, upon decimation, only attenuated $k\Lambda$ signals are aliased into the pilot/simulator bandwidth.

Quiet Mode

A filter algorithm been developed that has gain and phase characteristics that are compatible with real time computation. The filter reduces the aforementioned "noise" in the simulation model so significantly that it has been designated the "Quiet Mode Filter."

The basis for the Quite Mode Filter is a linear combination of classical notch filters, and a discrete realization technique that produces accurate responses. Because of the effectiveness of this combination, model performance is not influenced except to produce the desired attenuation in the regions of Λ, 2Λ, and 3Λ.

The filter may be routinely applied during I.C. mode for very clean states, permitting very good evaluations of such things as trim points and partial derivatives.

The filter is outlined as follows:

Where a very small damping factor is selected, ξ = 0.04, and where the selected frequencies are Λ multiples, as above, consider second-order Laplace factors given by classical notch filters, (j = 1, 2, 3),

$$f_j(s) = \frac{s^2 + (j\Lambda)^2}{s^2 + 2\xi j\Lambda s + (j\Lambda)^2}$$

and a linear combination given by the product of the first three factors,

$$f(s) = f_1(s)\, f_2(s)\, f_3(s)$$

The resultant filter f(s) attenuates the first three Λ multiples, provided a proper discrete implementation is used.

In view of the selected parameters and filter type, this represents a sensitive discrete realization problem, which is solved by using the "triangular (or trapezoidal) data hold." This technique is significant in that it neither advances the temporal index (avoiding a time shift) nor amplifies the gain in any region.

By using the triangular data hold the output is concurrent with the most recent, or current input, rather than advancing the output one cycle into the future. Hence, neither transport delay nor advance occurs. Unlike techniques such as the Bilinear Transform (Tustin), frequencies are not distorted; this is an especially important consideration for discrete realizations of notch filters.

The triangular data hold of a Laplace polynomial ratio f(s) may be obtained by use of the Newton-Gregory approximation (collating polynomial),

$$F(z) = Z\left[\left(\frac{1 - e^{-sT}}{s}\right)^2 \frac{e^{sT}}{T} f(s)\right]$$

where the resultant z-transform produces a recursion relationship that may then be programmed. This is a fairly complicated process for high order systems. For this reason generalized software has been developed at Ames Research Center to perform this function. The software creates z-transform solutions (difference equations) for ratios of polynomial Laplace transfer functions, similar to the zero-order hold software used at Ames for many years. The algorithms are based upon the theories of ref. 5.

The software permits the use of variable RPM in the simulation model. Providing that the "slowly varying coefficient hypothesis" is not violated, this means that the filter coefficients may be nonstationary.

The performance of the Quiet Mode Filter for a damping value of 0.04 is given in figure 6. The filter is shown to attenuate the 3N/rev frequency by a factor of about two-thirds, and attenuate 2N/rev and N/rev by even larger factors. The phase characteristics are excellent, and do not influence rotor system performance.

Figure 7 is presented for comparison with figures 2 and 5. In figure 7 the use of the Quiet Mode Filter is shown to attenuate the first three harmonics to such an extent that operate mode performance is effectively purged of spurious frequency content.

Dynamic Checks

Four separate dynamic checks are included in this report. These are (1) a longitudinal cyclic doublet (δ_e) in figures 8, 9 and 10; (2) a collective doublet (δ_c) in figures 11, 12 and 13; (3) a lateral cyclic doublet (δ_a) in figures 14, 15 and 16; and (4) a pedal doublet (δ_p) in figures 17, 18 and 19. These doublets are introduced using conventional helicopter controls.

Three figures are supplied for each control input. The first in a sequence of three figures shows the original model cycling at 20 msec, using neither subcycles nor the Quiet Mode Filter. The second in a sequence of three figures shows the influence of the subcycle technique.

Because of computational improvements that accrue using the subcycle technique, some noise reduction is observed. More significantly, maximum acceleration excursions are sometimes smaller, demonstrating that 20 msec is really not small enough for an accurate rotor simulation.

The third in a sequence of three figures shows the total system performance when both the subcycle technique and the Quiet Mode Filter are used. The acceleration histories in this figure differ from those of the second figure (in a sequence) only in that aliased frequencies are further attenuated.

In figures 8, 9 and 10 the vehicle acceleration histories are shown in response to a longitudinal cyclic (pitch) input. The same scales and total model (20-msec) cycle time are used in each of three sequential figures, for illustrating the results of this research. The selected example (an 80 knot, level-flight configuration with small control deflections) produces rather benign vehicle dynamics, so that extreme excursions and harmonics do not overwhelm the pertinent data.

In figure 8 the original model acceleration histories are shown, where neither the subcycle technique nor the quiet mode filter was used. In this figure the predicted aliased harmonics are shown in those traces with sufficiently small ordinate limits.

In figure 9 the subcycle technique was used. This means that although the model cycled at 20 msec, the blade loop within the rotor model cycled three times as fast (subcycle loop). Decimation occurs at the rotor-model output boundary, where communication is made with other subsystems in the model. In this example it is most convenient to think of the interface as being equivalent to using only the third output from the rotor system.

It should be noticed that the subcycle technique alone produces cleaner traces, even though the model and plot output period is the same (20 msec). This should be no surprise to those familiar with the algebraic loops and nonlinearities in rotor models. Generally, running a nonlinear (sub)model fast and then observing outputs at a slower frequency is more accurate than simply running and observing the model at a slow frequency. This phenomenon may be observed in the maximum lateral acceleration (V_{BD}) variations in a comparison of figure 8(b) with 9(b).

In figure 9, however, for certain linear and rotational states, the aliased harmonic multiples are shown to persist. This is especially true in yaw acceleration, where the nonlinear lag damper has previously been shown to create energetic harmonics (ref. 4).

In figure 10 both the subcycle technique and quiet mode filters are used. As postulated, while aliased harmonics are suppressed the dynamic responses are preserved.

The missing figure in this sequence, wherein the quiet mode filter is used but the subcycle technique is not, is actually an invalid option. A discrete realization of a linear filter that attempts to attenuate frequencies above the Nyquist limit cannot magically reach into the bandwidth and attenuate them at the aliased location.

In figures 11, 12 and 13 the vehicle acceleration histories are shown in response to a collective (vertical) input. The lateral acceleration response shows significant differences when figure 11(b) is compared with 12(b). The transition to figure 13(b) is then quite reasonable.

In figures 14, 15 and 16 the vehicle acceleration histories are shown in response to a lateral cyclic (roll) input. In the longitudinal acceleration (U_{BD}) traces the signal is nicely separated from noise in the transition from figure 14(a) to 16(a).

In figures 17, 18 and 19 the vehicle acceleration histories are shown in response to a pedal (yaw) input. This input does not excite the rotor system as much as do the other inputs.

Reconstruction

The N/rev signal is sometimes useful in simulation, but not for obscuring vehicle responses, and certainly not for driving large-scale motion devices. Studies involving the determination of pilot fatigue, for instance, should properly use a seat shaker to generate this harmonic; drive motors for large-scale motion devices should not be subjected to steady-state signals beyond their bandwidth.

The N/rev signal may be reconstructed. As inputs to the quiet-mode filter, the nonattenuated signals may be used to determine the magnitude of the N/rev harmonic by use of an algorithm with a small spectral window. Of course, the N/rev frequency value is itself always known by observing the RPM. Then, using an *analog* device for creating the N/rev drive frequency, a small-motion device (seat shaker) may be used for superimposing the proper signals.

For example, by assuming a subcycle (every ΔT) data sequence of the form,

$$y_k = A + B\cos(k\Lambda\Delta T) + C\sin(k\Lambda\Delta T)$$

it may be easily shown that the magnitude of the N/rev harmonic is given to a good approximation (with only one subcycle of pure transport delay) by use of the formula,

$$M_k = \frac{[D_k]^{\frac{1}{2}}}{(1 - \cos\Lambda\Delta T)[2(1 + \cos\Lambda\Delta T)]^{\frac{1}{2}}}$$

where the numerator term is a function of the current and two previous data values,

$$D_k = y_k^2 + y_{k-2}^2 + y_k y_{k-2}\cos\Lambda\Delta T + 2y_{k-1}(1 + \cos\Lambda\Delta T)(y_{k-2} - y_{k-1} - y_k)$$

Note that by acquiring D_k each ΔT, the computation of M_k (including the square root operations) need only be performed every $T = m\Delta T$ for input/output communication.

Conclusions

In real-time simulation, whenever there is a disparity in computer speed relative to model workload, the subcycle technique is valuable for the generation of correct rotor dynamics. Rotor dynamics, however, include high frequency harmonics.

These high frequency harmonics alias into the bandwidth in accordance with the aliasing equation, and this phenomenon occurs *at all communication points*, including module-to-module transfers and computer input/output.

The Quiet Mode Filter is especially valuable in attenuating these distinct frequencies *before they alias* into the low frequency bandwidth.

Simulations using these techniques will not be contaminated with the spurious frequencies that obscure time histories, create variable trim points, and produce erroneous stability and control derivative data.

References

1. Houck, Jacob A., *et al:* Rotor Systems Research Aircraft Simulation Mathematical Model. NASA TM-78629, November, 1977.

2. Howlett, J. J.: UH-60A Black Hawk Engineering Simulation program, Vol. I - Mathematical Model. NASA CR-166309, 1981.

3. Houck, Jacob A.: Computational Aspects of Real-Time Simulation of Rotary-Wing Aircraft. NASA CR-147932, May 1976.

4. McFarland, R. E.: The N/Rev Phenomenon in Simulating a Blade-Element Rotor System. NASA TM 84344, March 1983.

5. McFarland, R. E.; and Rochkind, A. B.: On Optimizing Computations for Transition Matrices. IEEE Trans. Automatic Control, Vol. AC-23, No. 3, June 1978.

APPENDIX A

Blade Summations

This appendix develops relationships that demonstrate the spectral selection process of trigonometric expansions of rotor variables when they are summed over the blade index, n.

Providing only that a rotor system consists of N equally-spaced blades, the azimuth angle of the n^{th} blade in a mathematical model of the system may be given by (n = 1, 2, ... N),

$$\psi_n = \psi + 2\pi(n - 1)/N$$

where the azimuth angle of the first blade for reference purposes is defined by the integral of the rotor speed Ω (rad/sec),

$$\psi = \int_0^t \Omega dt$$

Considering blades with identical physical properties (length, mass distribution, etc.), harmonic expansions of rotor system variables may be expressed in terms of trigonometric functions of harmonic multiples "i" of the azimuth angle, and RPM-independent parameters (here lumped into coefficient terms). For example, flapping or lagging angle representations are often written in Fourier form, where infinite series are truncated beyond some index value. Hence, for a general treatment of the frequency content of rotor quantities, consider the blade-level Fourier representation of an arbitrary blade-level variable F_n:

$$F_n = \sum_{i \geq 0} [\, g_i \cos(i\psi_n) + h_i \sin(i\psi_n) \,]$$

The harmonic expansion of a blade variable reveals its spectral components. At the "rotor system level" of modeling, however, the expression must be summed over the blade index ($1 \leq n \leq N$), and this operation has spectral consequences.

The summation operation over the blade index produces the phenomenon of spectral filtering; it influences all rotor system outputs. The mathematical steps that produce this phenomenon are presented below. Using integer multiples (harmonics, i) of the azimuth angle, trigonometric functions involving the index of summation (n) are separated:

$$\sin(i\psi_n) = \sin(i[\psi + 2\pi(n - 1)/N])$$

$$= \sin(2\pi in/N)[\cos(i\psi)\cos(2\pi i/N) + \sin(i\psi)\sin(2\pi i/N)]$$

$$+ \cos(2\pi in/N)[\sin(i\psi)\cos(2\pi i/N) - \cos(i\psi)\sin(2\pi i/N)]$$

$$\cos(i\psi_n) = \cos\{i[\psi + 2\pi(n-1)/N]\}$$

$$= \sin(2\pi in/N)[\cos(i\psi)\sin(2\pi i/N) - \sin(i\psi)\cos(2\pi i/N)]$$

$$+ \cos(2\pi in/N)[\sin(i\psi)\sin(2\pi i/N) + \cos(i\psi)\cos(2\pi i/N)]$$

From these expressions, the summing process over the blade index "n" requires only the two series,

$$\sum_{n=1}^{N} \sin(2\pi in/N) = \frac{\cos(\pi i/N) - \cos(2\pi i)\cos(\pi i/N) + \sin(2\pi i)\sin(\pi i/N)}{2\sin(\pi i/N)}$$

$$\sum_{n=1}^{N} \cos(2\pi in/N) = \frac{\sin(2\pi i)\cos(\pi i/N) + \cos(2\pi i)\sin(\pi i/N) - \sin(\pi i/N)}{2\sin(\pi i/N)}$$

Providing that $i/N \neq m$ (where m is any integer), these sums both vanish. Also, when $i/N = m$, the sine series vanishes. When $i/N = m$, however, the cosine series is equal to N.

This leads to the important fact that whenever the ratio $i/N = m$, the harmonic azimuth angle summations are given by

$$\sum_{n=1}^{N} \sin(i\psi_n) = N\sin(mN\psi)$$

(where $i/N = m$)

$$\sum_{n=1}^{N} \cos(i\psi_n) = N\cos(mN\psi)$$

whereas both sums vanish whenever i/N is not equal to an integer. The summations illustrate that for simple trigonometric relationships all harmonic terms, except for multiples of the number of blades, vanish when summed over the blade index.

In order to use this phenomenon, recall that the coefficients are independent of azimuth angle. In summing over the blade index the summation operations (n, i) may then be interchanged. Using the above results, this produces a summed function that contains only N/rev multiples in its frequency content:

$$\sum_{n=1}^{N} F_n = N \sum_{i=0}^{\infty} [\, g_{iN}\cos(iN\psi) + h_{iN}\sin(iN\psi) \,]$$

Similarly, resolutions of blade level functions summed over the blade index (where $N \geq 3$, here due to notation limitations) also produce only N-per-rev frequency content, *e.g.*,

$$\sum_{n=1}^{N} F_n\sin\psi_n = \tfrac{1}{2}N \sum_{i=0}^{\infty} \{\, [g_{iN+1} - g_{iN-1}]\cos(iN\psi) - [h_{iN+1} - h_{iN-1}]\sin(iN\psi) \,\}$$

$$\sum_{n=1}^{N} F_n\cos\psi_n = \tfrac{1}{2}N \sum_{i=0}^{\infty} \{\, [g_{iN+1} + g_{iN-1}]\cos(iN\psi) + [h_{iN+1} + h_{iN-1}]\sin(iN\psi) \,\}$$

$$\sum_{n=1}^{N} F_n\sin^2\psi_n = \tfrac{1}{4}N \sum_{i=0}^{\infty} \{\, [2g_{iN} - g_{iN+2} - g_{iN-2}]\cos(iN\psi) - [2h_{iN} - h_{iN+2} - h_{iN-2}]\sin(iN\psi) \,\}$$

$$\sum_{n=1}^{N} F_n\cos^2\psi_n = \tfrac{1}{4}N \sum_{i=0}^{\infty} \{\, [2g_{iN} + g_{iN+2} + g_{iN-2}]\cos(iN\psi) + [2h_{iN} + h_{iN+2} + h_{iN-2}]\sin(iN\psi) \,\}$$

$$\sum_{n=1}^{N} F_n\sin\psi_n\cos\psi_n = \tfrac{1}{4}N \sum_{i=0}^{\infty} \{\, [g_{iN-2} - g_{iN+2}]\sin(iN\psi) - [h_{iN+2} - h_{iN-2}]\cos(iN\psi) \,\}$$

This illustrates the spectral filtering phenomenon that occurs in a rotor system model. Only "N-tuples" of the azimuth angle survive under summation. All forces and moments contain terms such as these at the rotor system level of computation; if their frequency content is higher than the Nyquist limit, it is aliased into the discrete bandwidth.

APPENDIX B

Blade Integrations

The integration algorithms used for the Sikorsky nonlinear blade-element rotor models are discussed here. These integration algorithms have the unusual characteristic of being tuned to the rotor speed only, and tend to modify responses both above and below this frequency. This fact has both good and bad consequences. It is important to realize, however, that at the blade level of computation the rotor speed is indeed the dominant frequency, and that this is caused by the basic physics of the system. The rotor-system-transfer-function characteristics, for instance, play a subordinate roll, as does hub motion and pilot input. For both flapping (β) and lagging (δ) angles, the integration algorithms may be expressed by

$$\dot{\beta}_n(k) = \dot{\beta}_n(k-1)\cos(\Delta\psi) + \ddot{\beta}_n(k-1)\sin(\Delta\psi)/\Omega$$

$$\beta_n(k) = \beta_n(k-1) + [\,\dot{\beta}_n(k) + \dot{\beta}_n(k-1)\,]\tan(\Delta\psi/2)/\Omega$$

At the blade level of computation these integration processes are highly correlated, *e.g.*,

$$\beta_n(k) = f\,[\,\beta_n(k), \dot{\beta}_n(k), \delta_n(k), \dot{\delta}_n(k)\,]$$

and rotor system outputs are sensitive to each of these variables. Their relative gain and phase characteristics are thus important to the computation of rotor system forces and torques.

For each blade, the following z-transform relationships describe the integration processes:

$$I_n(z) = \frac{\dot{\beta}_n(z)}{\ddot{\beta}_n(z)} = \frac{\sin(\Delta\psi)}{\Omega[z - \cos(\Delta\psi)]}$$

$$J_n(z) = \frac{\beta_n(z)}{\dot{\beta}_n(z)} = \frac{\tan(\Delta\psi/2)[z + 1]}{\Omega[z - 1]}$$

and their product, or "double integration,"

$$K_n(z) = \frac{\beta_n(z)}{\ddot{\beta}_n(z)} = \frac{[1 - \cos(\Delta\psi)][z + 1]}{\Omega^2[z - 1][z - \cos(\Delta\psi)]}$$

From these z-transforms, the log magnitudes and phase angles may be computed, and compared to the perfect (continuum) integration processes. This is presented in figure 20, where the longer dashed lines denote perfect linear performance. The solid lines display the discrete performance when the cycle time is 20 msec, and the shorter dashed lines are used to show the performance improvement when the subcycle procedure is used. In this case m = 3 subcycles are required, making the effective blade-level cycle time equal to 6.67 msec (20/3).

In figure 20 a variety of things may be noted. In 20(a) we see that in the integration of blade accelerations the resultant velocity frequencies above the rotor speed are *amplified*, and thus contribute "noise" to the rotor system outputs. Their relative phase error leaves much to be desired. The positional contribution relative to acceleration is shown in 20(c). Here we see that high frequency attenuation occurs, which is usually desirable in discrete simulation, but it does nothing for our confidence in the magnitudes of N/rev multiples. Further, the phase relationship shown in figure 20(e) is bad.

Consider the consequence of aliasing in view of the integration magnitudes. Using a cycle time of 6.67 msec the 3N/rev signal at about 51 Hz would have a very small gain through any of the integration processes. However, when a cycle time of 20 msec is used, this signal appears *in the computations* at about 1.6 Hz, with considerable gain amplification.

In real time simulation a cycle time should be used where computations are independent of small cycle time variations. If results are a function of cycle time, then the computations certainly do not simulate the continuum. For a nonlinear rotor system model, these integration algorithms show that aliased harmonics do indeed influence responses when the cycle time is in the neighborhood of 20 msec, despite the fact that the algorithms are themselves "tuned" to the primary blade forcing function frequency Ω.

Figure 20 demonstrates that rotor responses are degraded when cycle times on the order of 20 msec are used. Then subcycle technique, however, producing an effective rotor-system cycle time one third the size of the original, is seen to produce considerable improvement in both magnitude and phase.

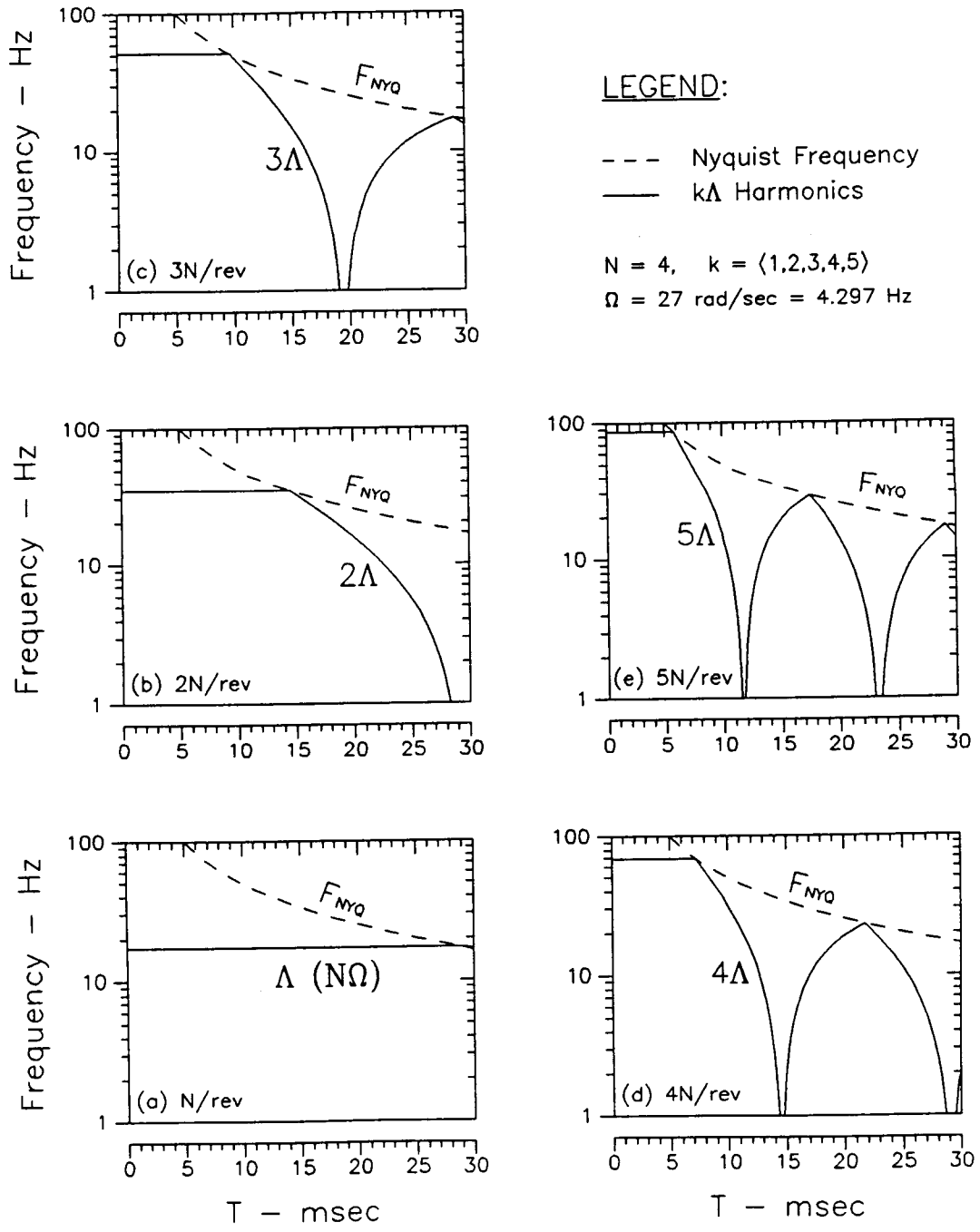

Figure 1.– Aliasing of rotor harmonics.

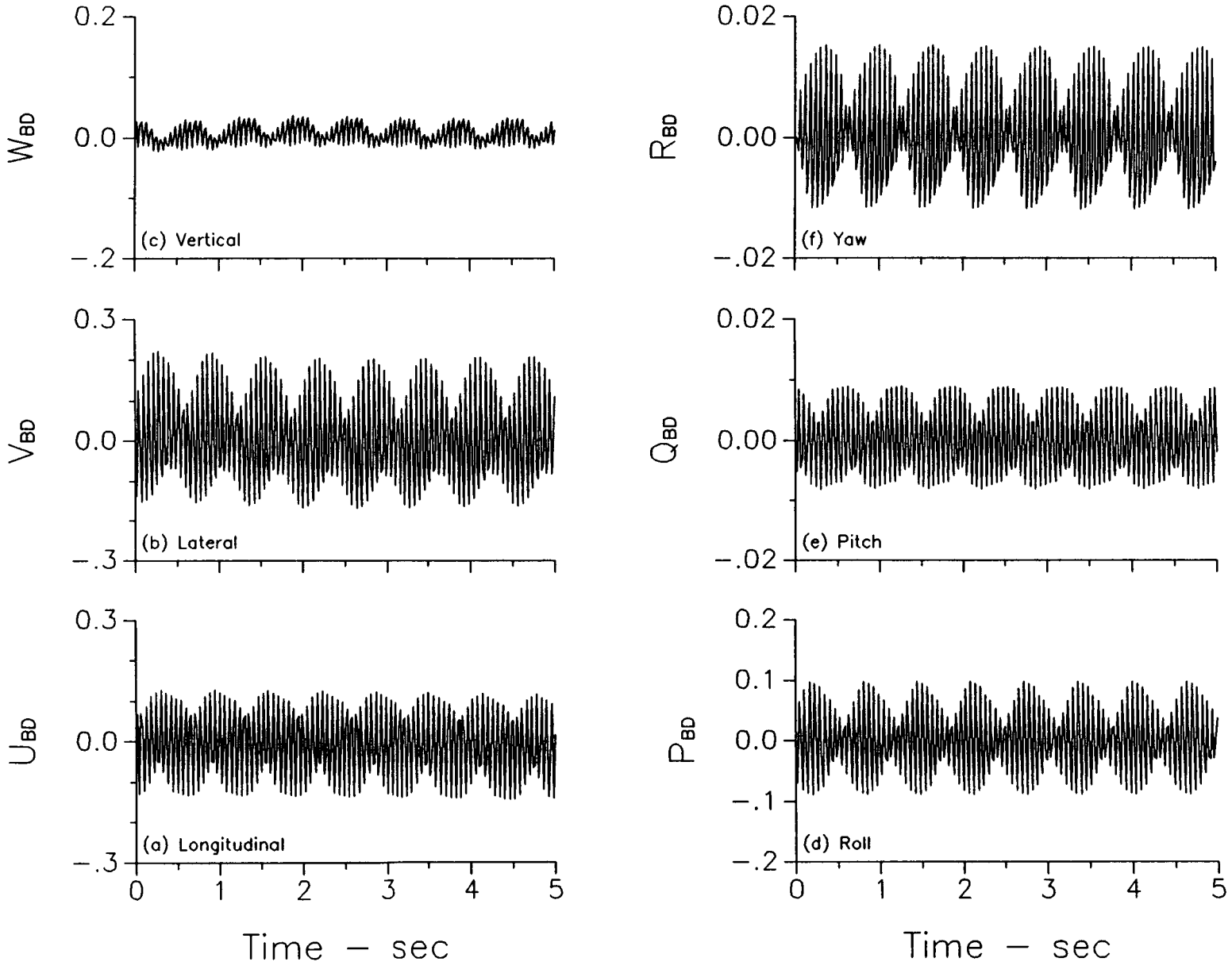

Figure 2.– Vehicle accelerations with neither subcycles nor filters (T = 20 msec).

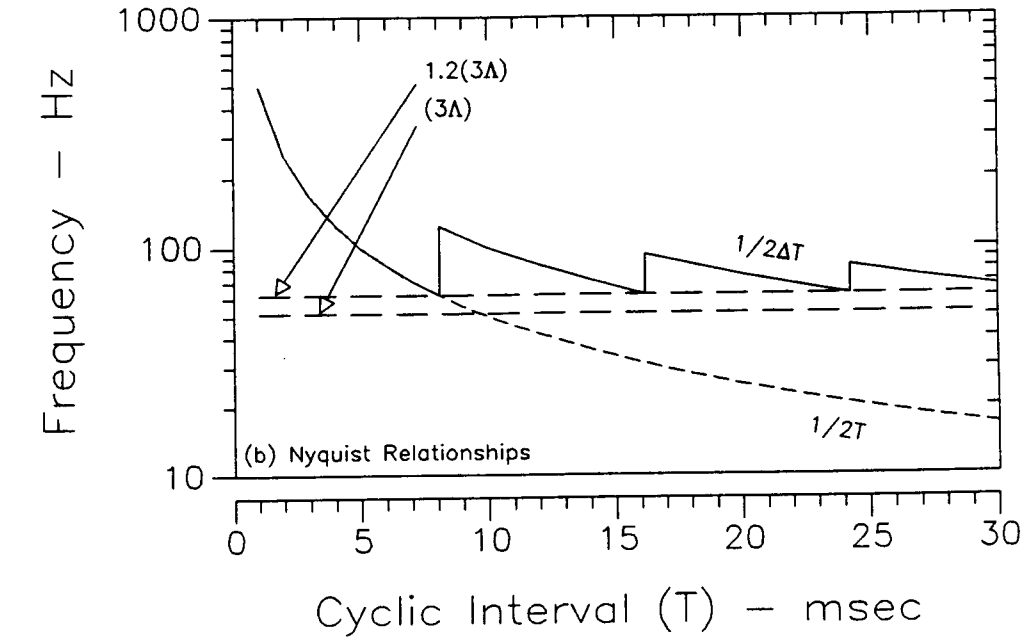

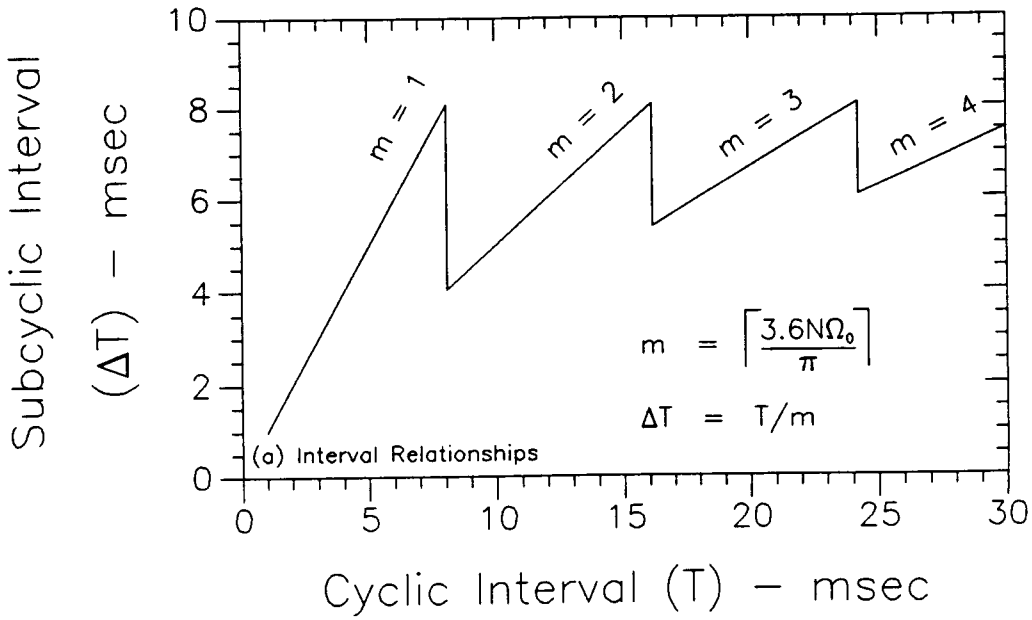

Figure 3.– Subcycles vs cycles.

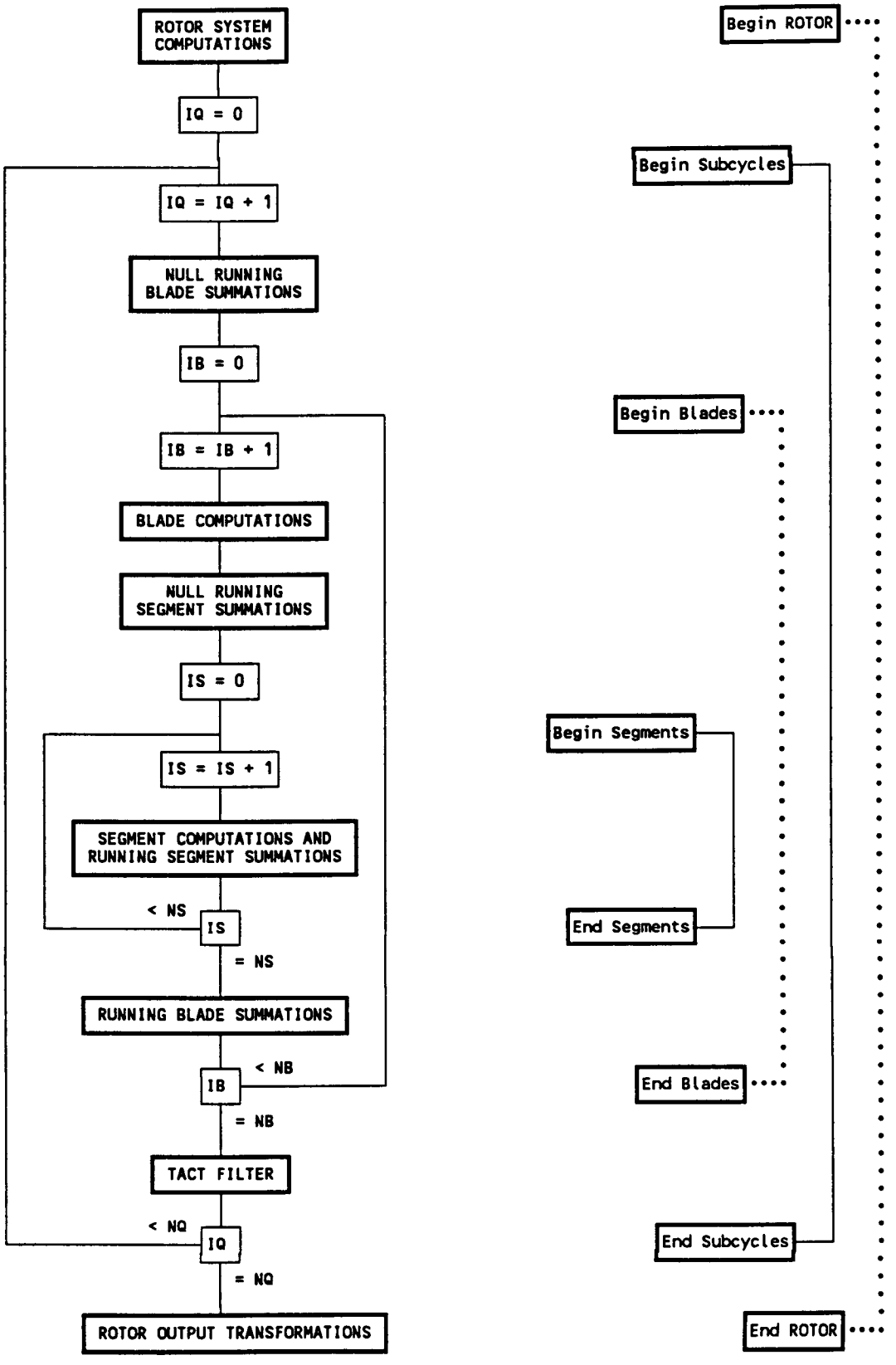

Figure 4.– Rotor subprogram structure.

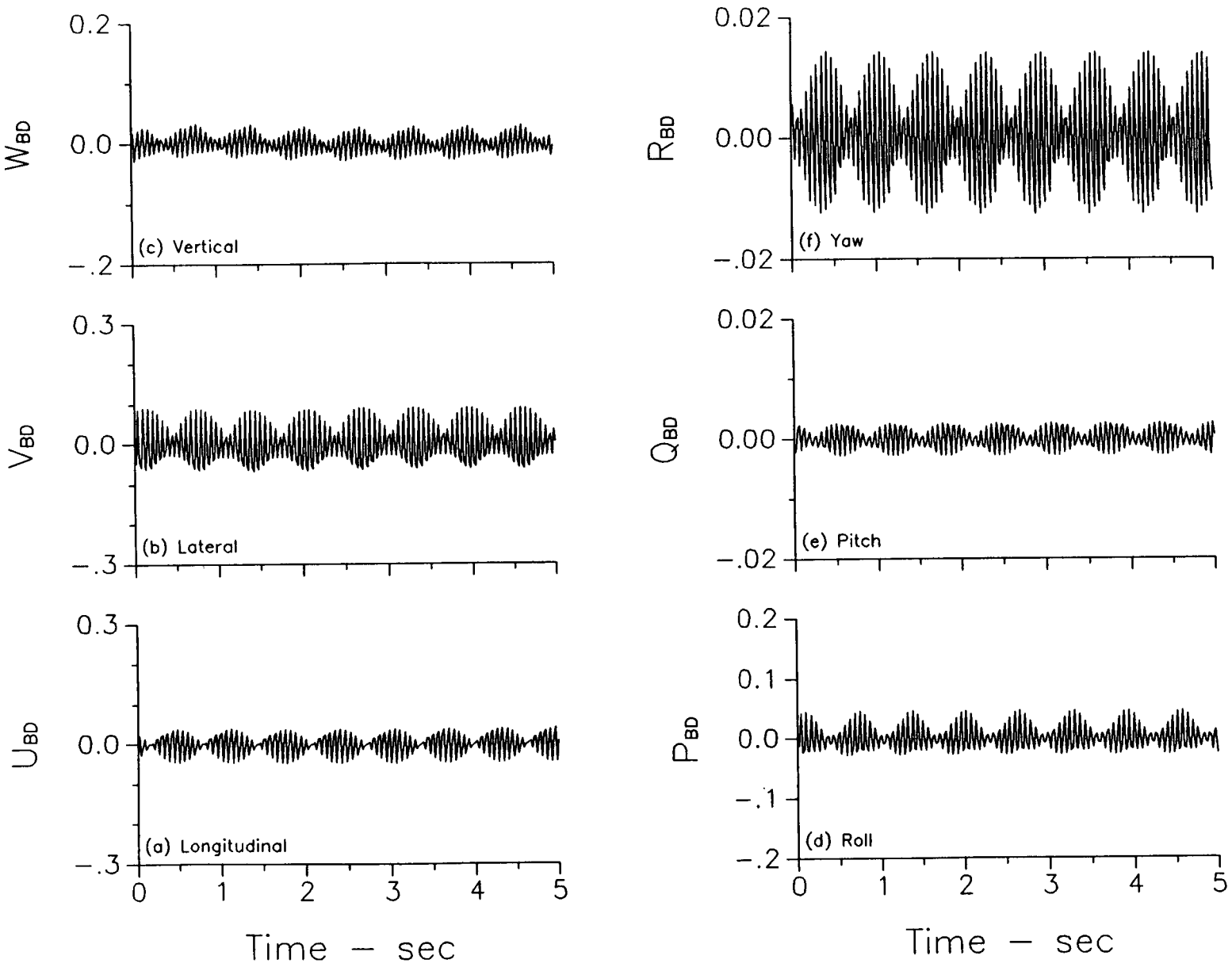

Figure 5.– Vehicle accelerations with subcycles but without filters (T = 20 msec).

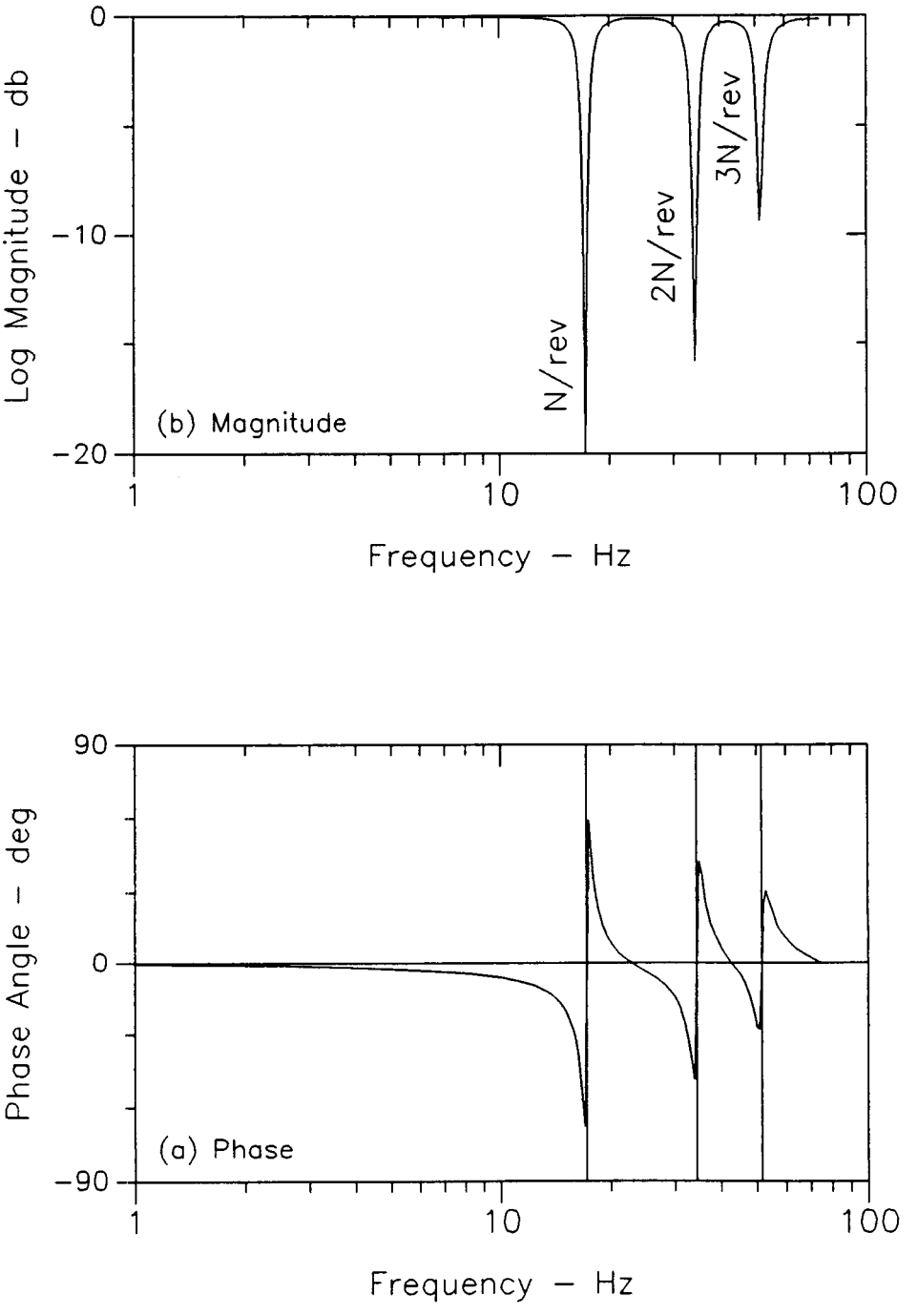

Figure 6.– Triple notch filter, $\zeta = 0.04$.

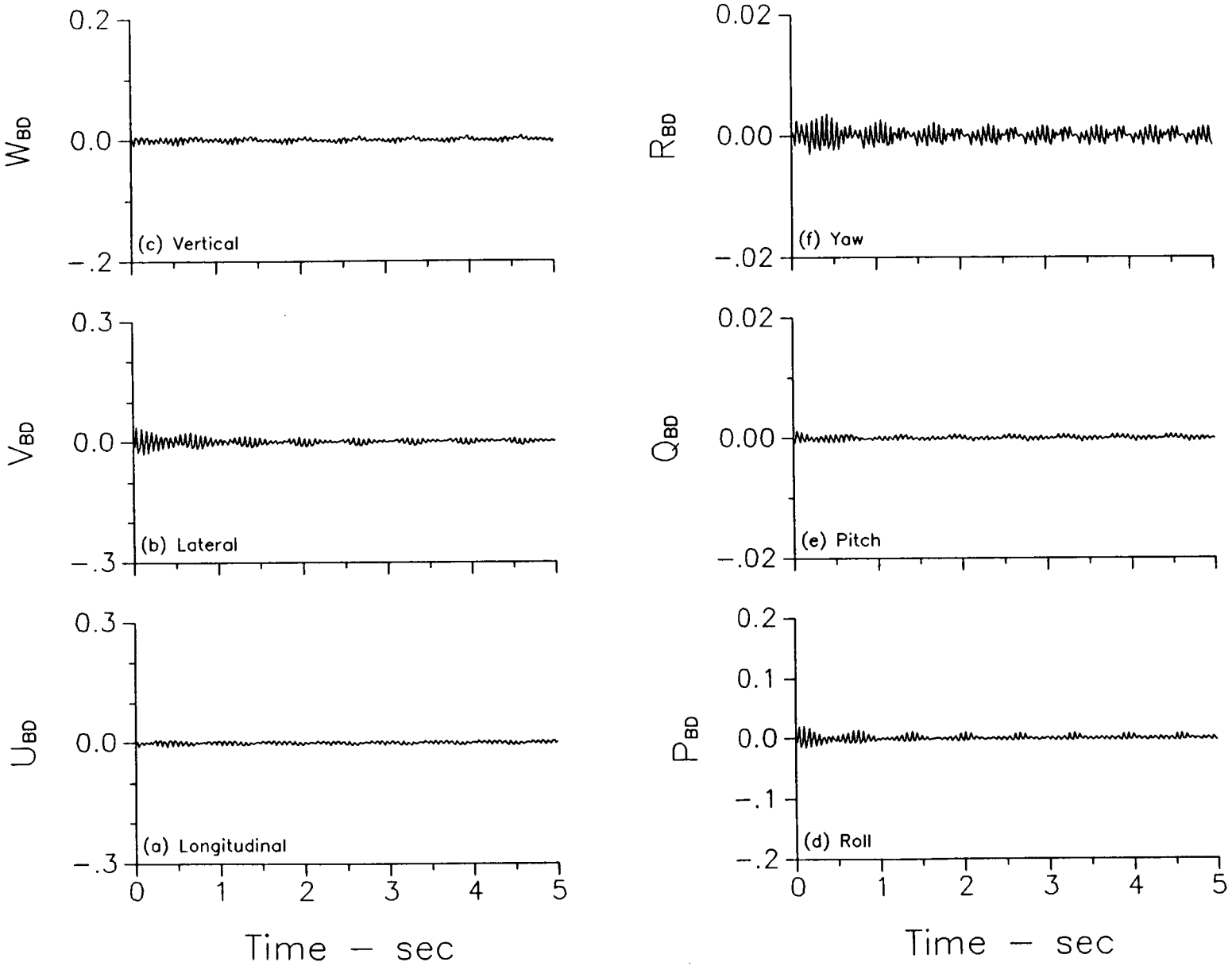

Figure 7.– Vehicle accelerations with both subcycles and filters (T = 20 msec).

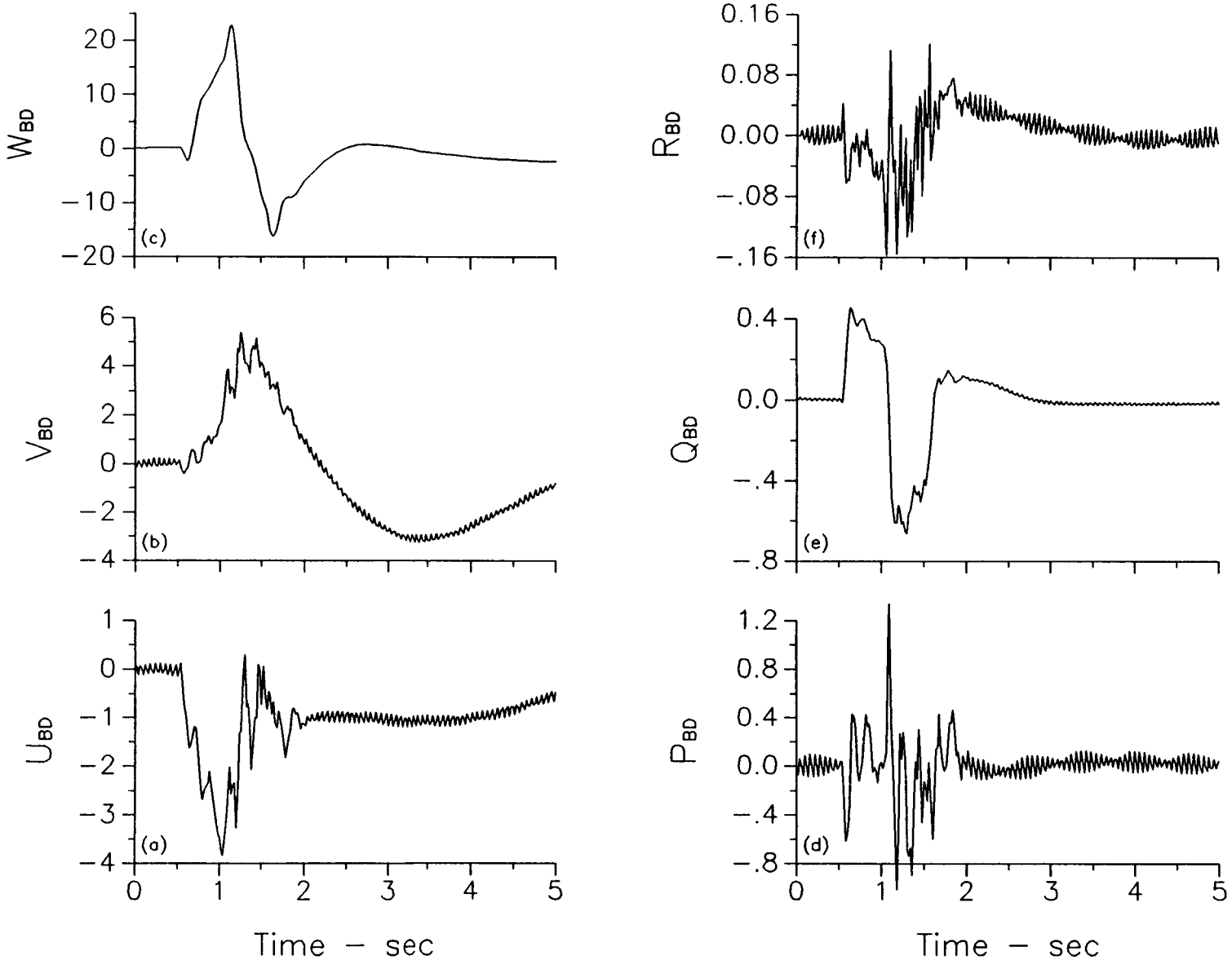

Figure 8.– Pitch (δ_e^i) dynamic check original system.

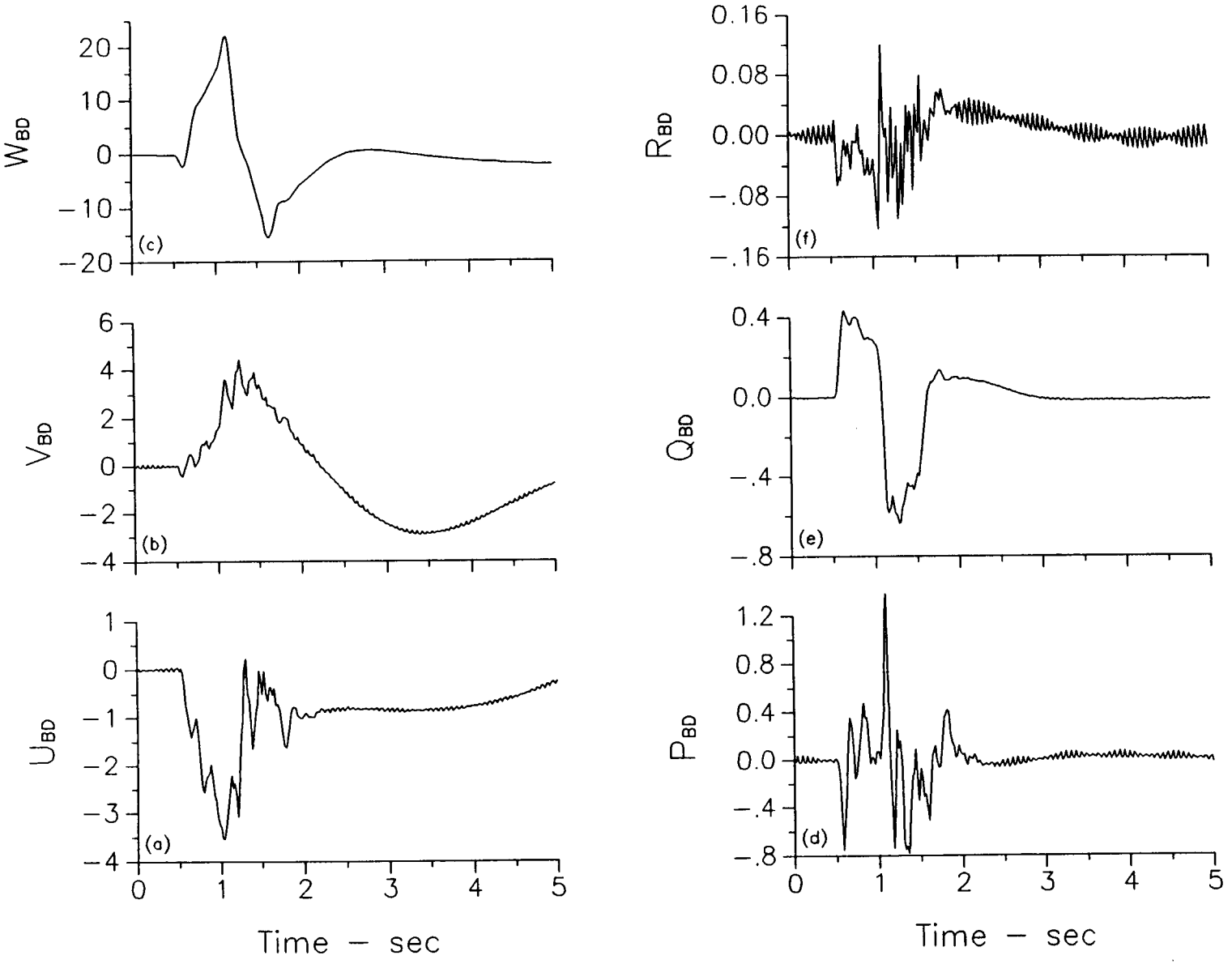

Figure 9.– Pitch (δ_e) dynamic check using subcycles.

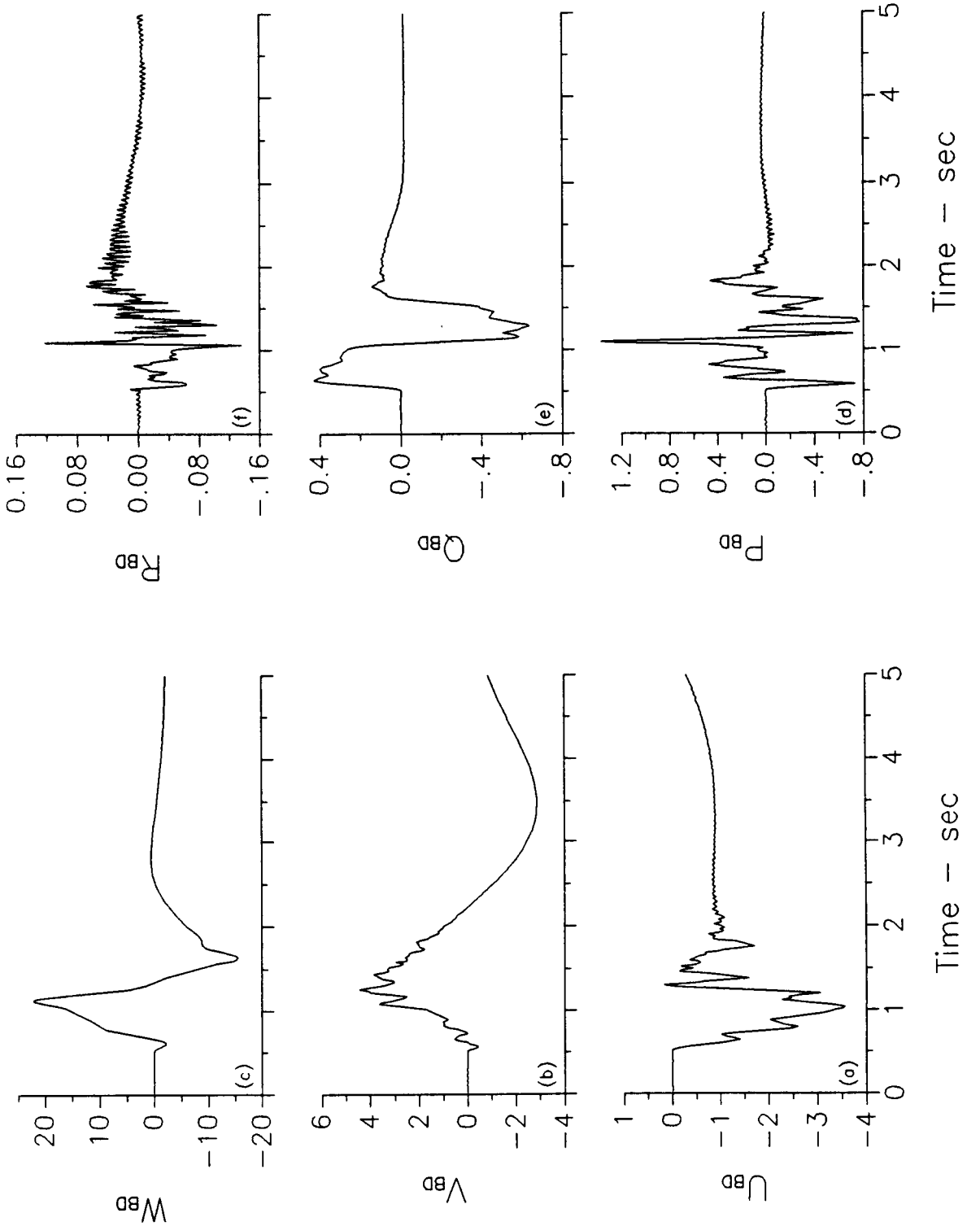

Figure 10.- Pitch (δ_e) dynamic check using subcycles and quiet mode.

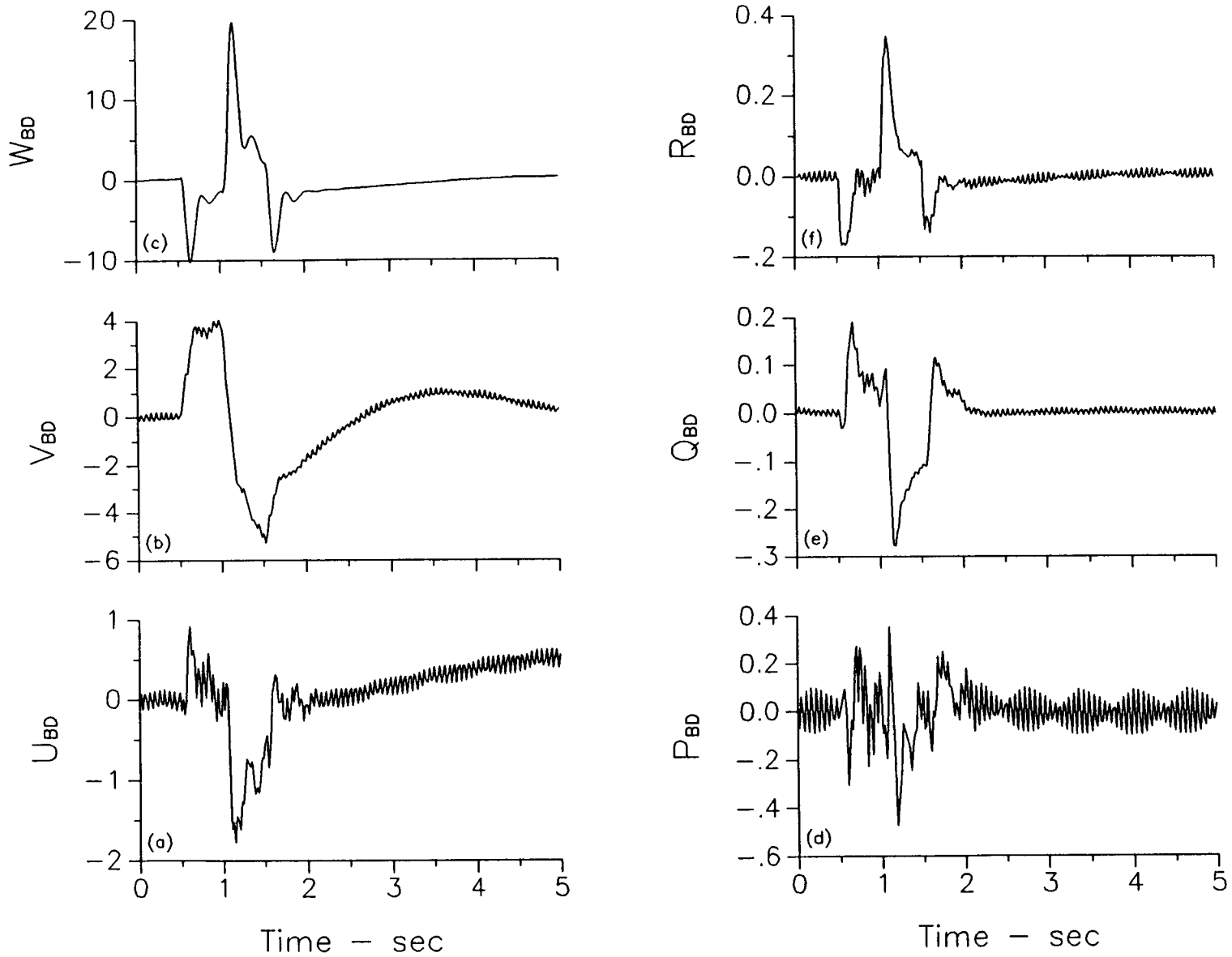

Figure 11.– Collective (δ_c) dynamic check original system.

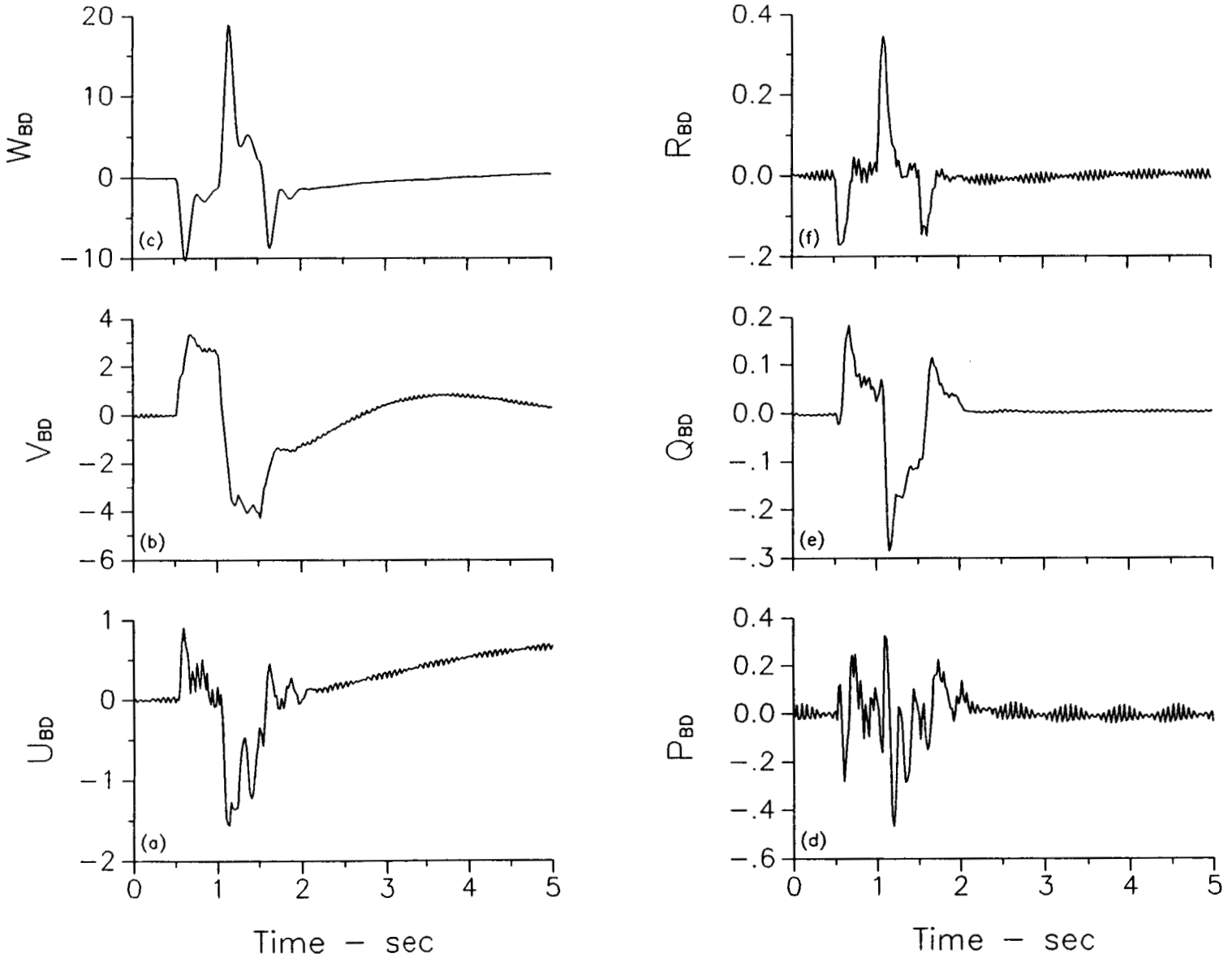

Figure 12.– Collective (δ_c) dynamic check using subcycles.

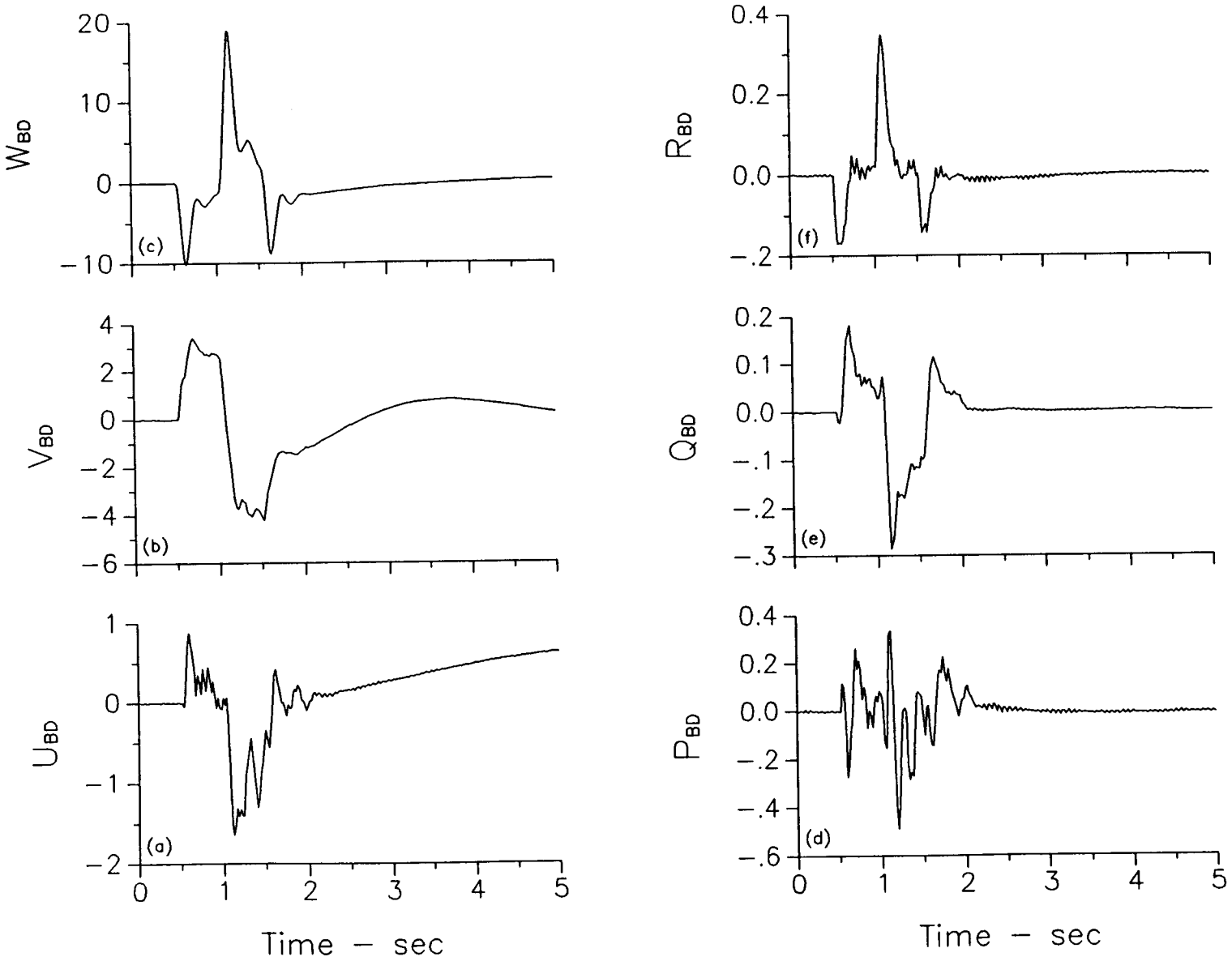

Figure 13.– Collective (δ_c) dynamic check using subcycles and quiet mode.

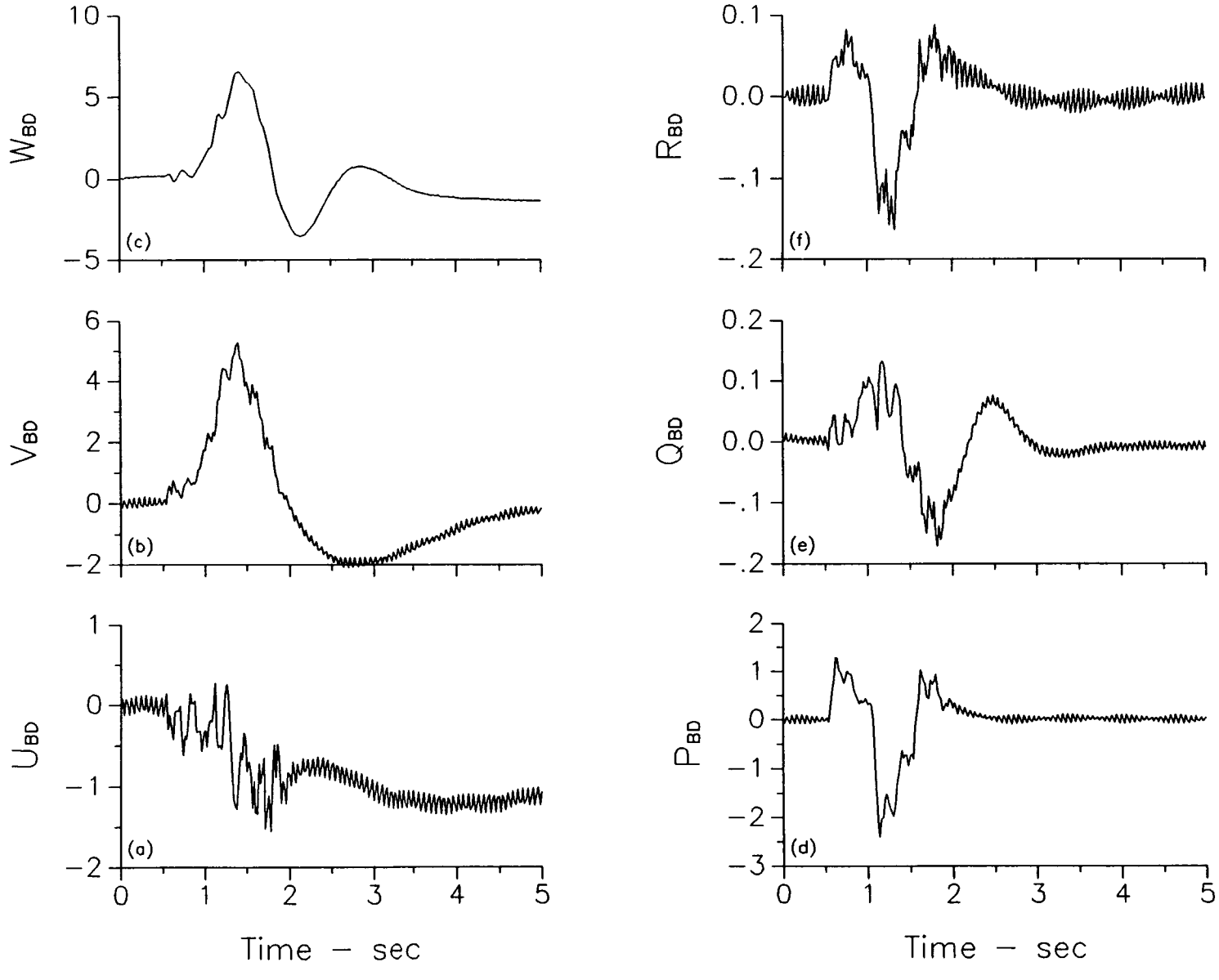

Figure 14.– Roll (δ_a) dynamic check original system.

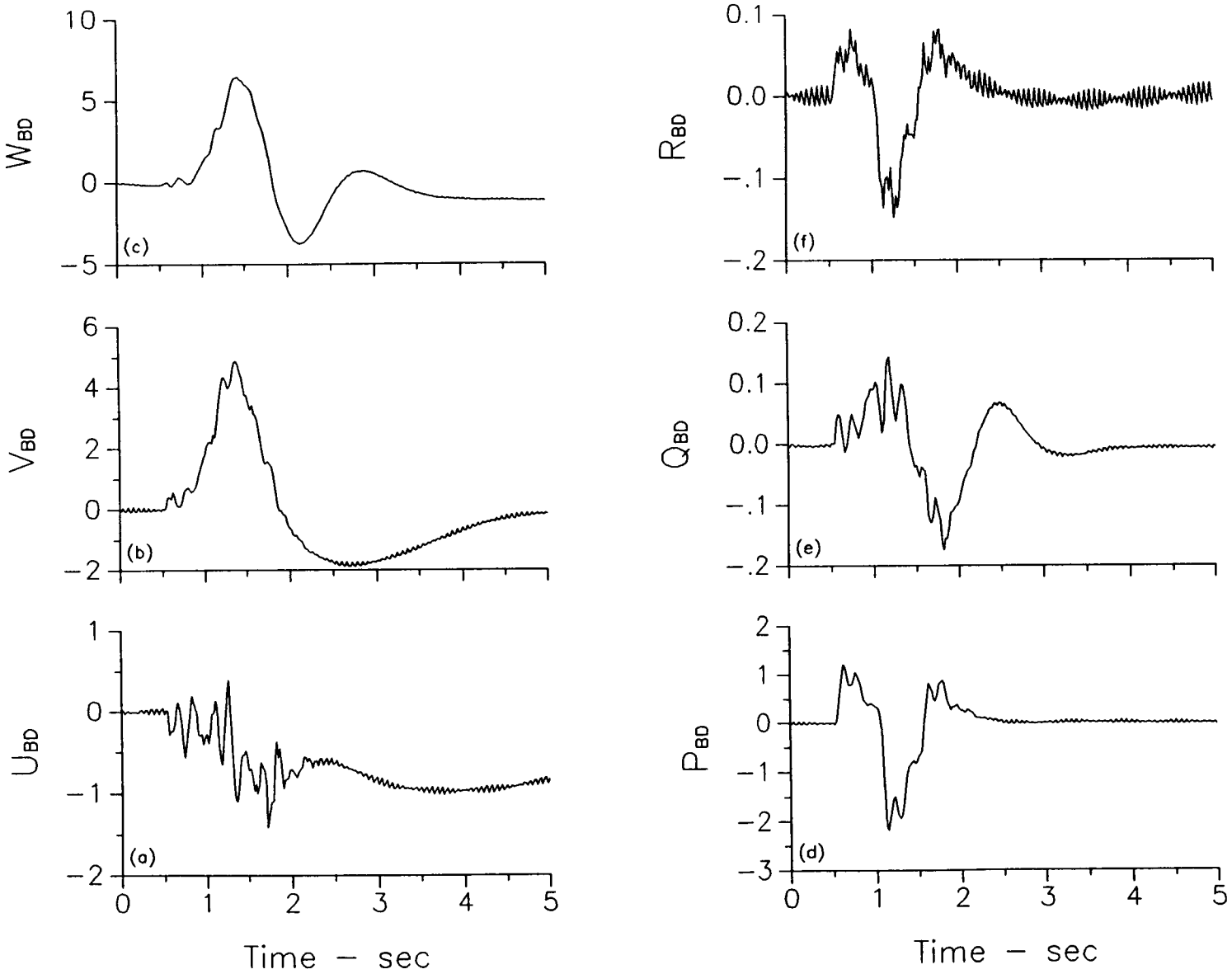

Figure 15.– Roll (δ_a) dynamic check using subcycles.

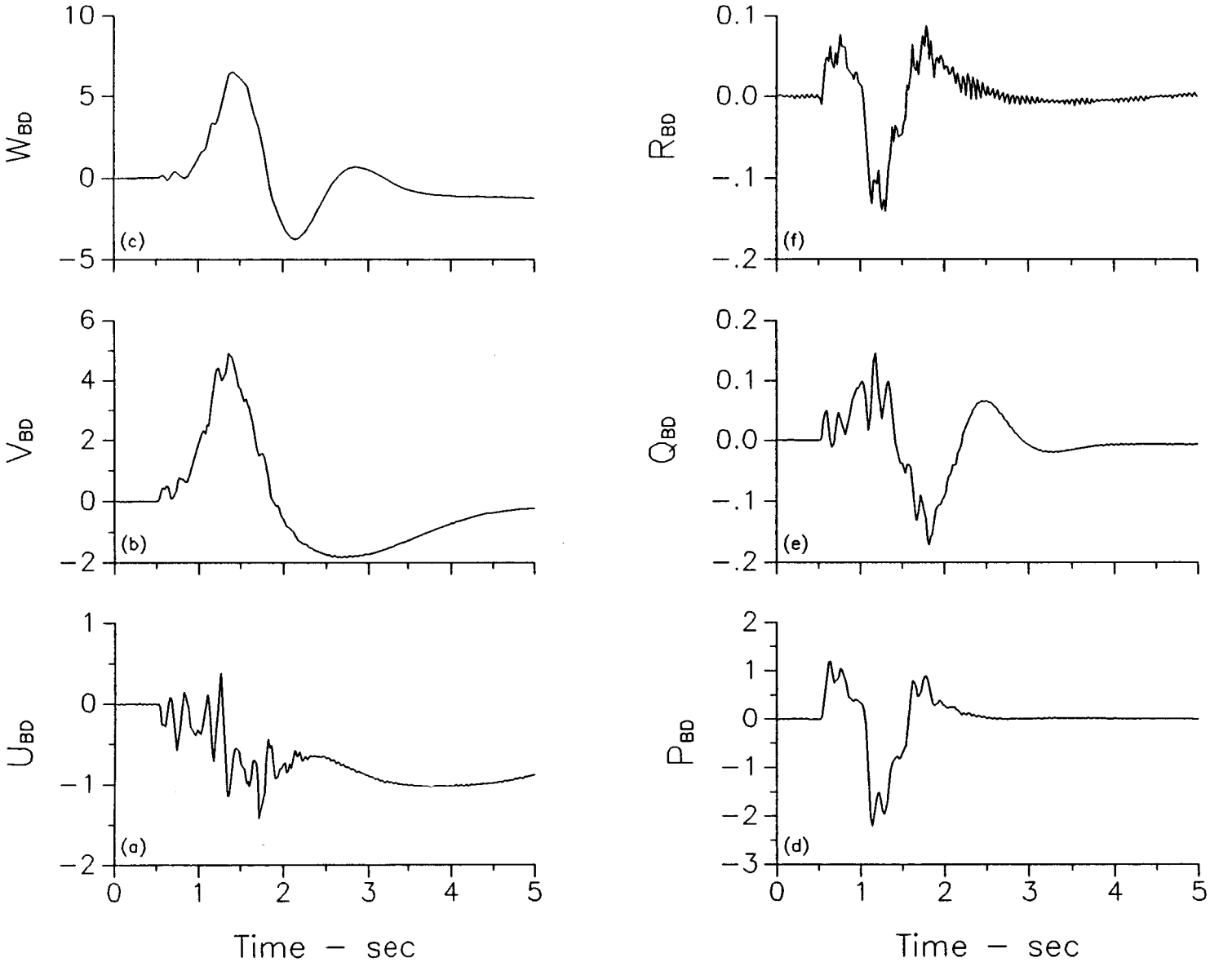

Figure 16.– Roll (δ_a) dynamic check using subcycles and quiet mode.

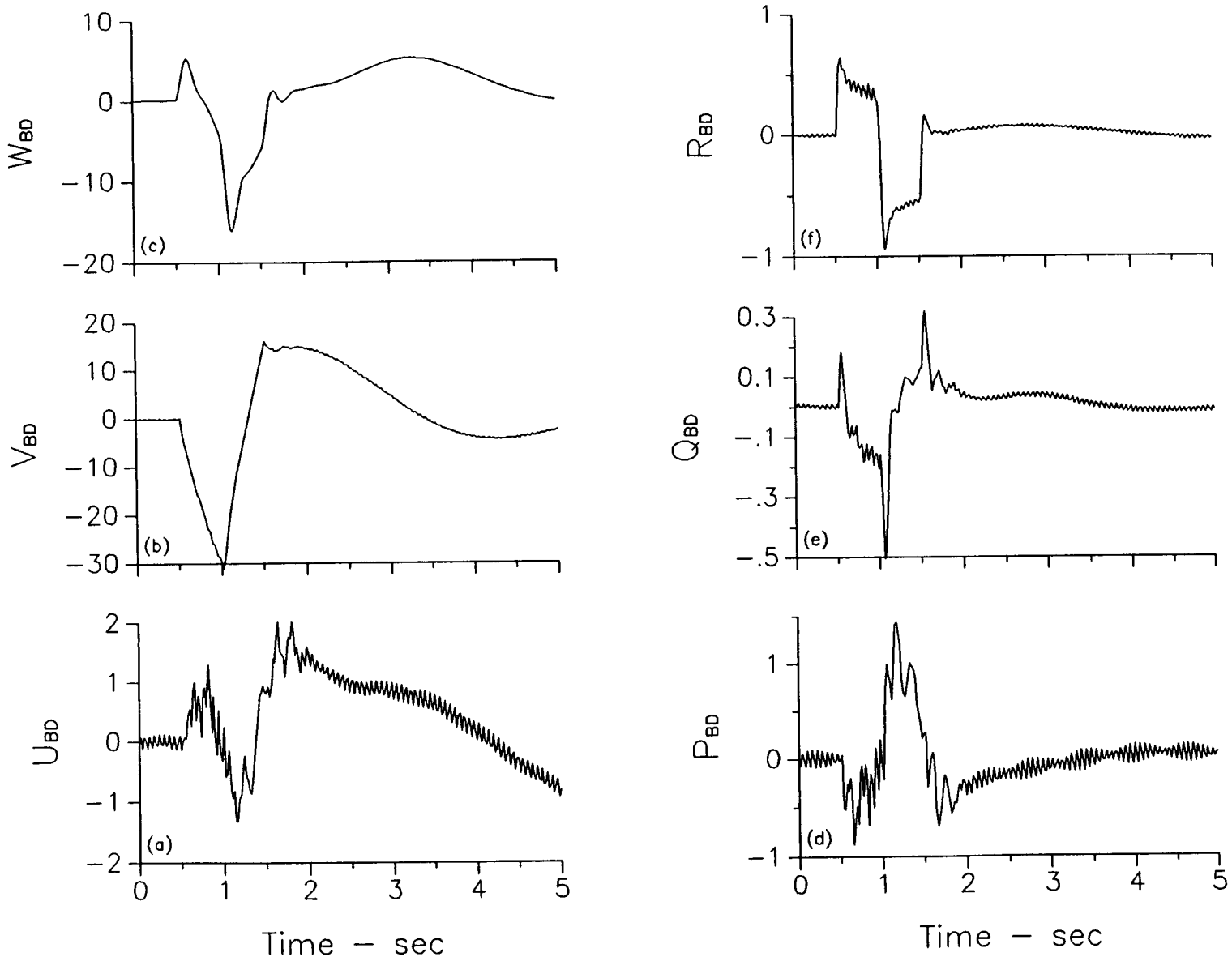

Figure 17.– Pedal (δ_p) dynamic check original system.

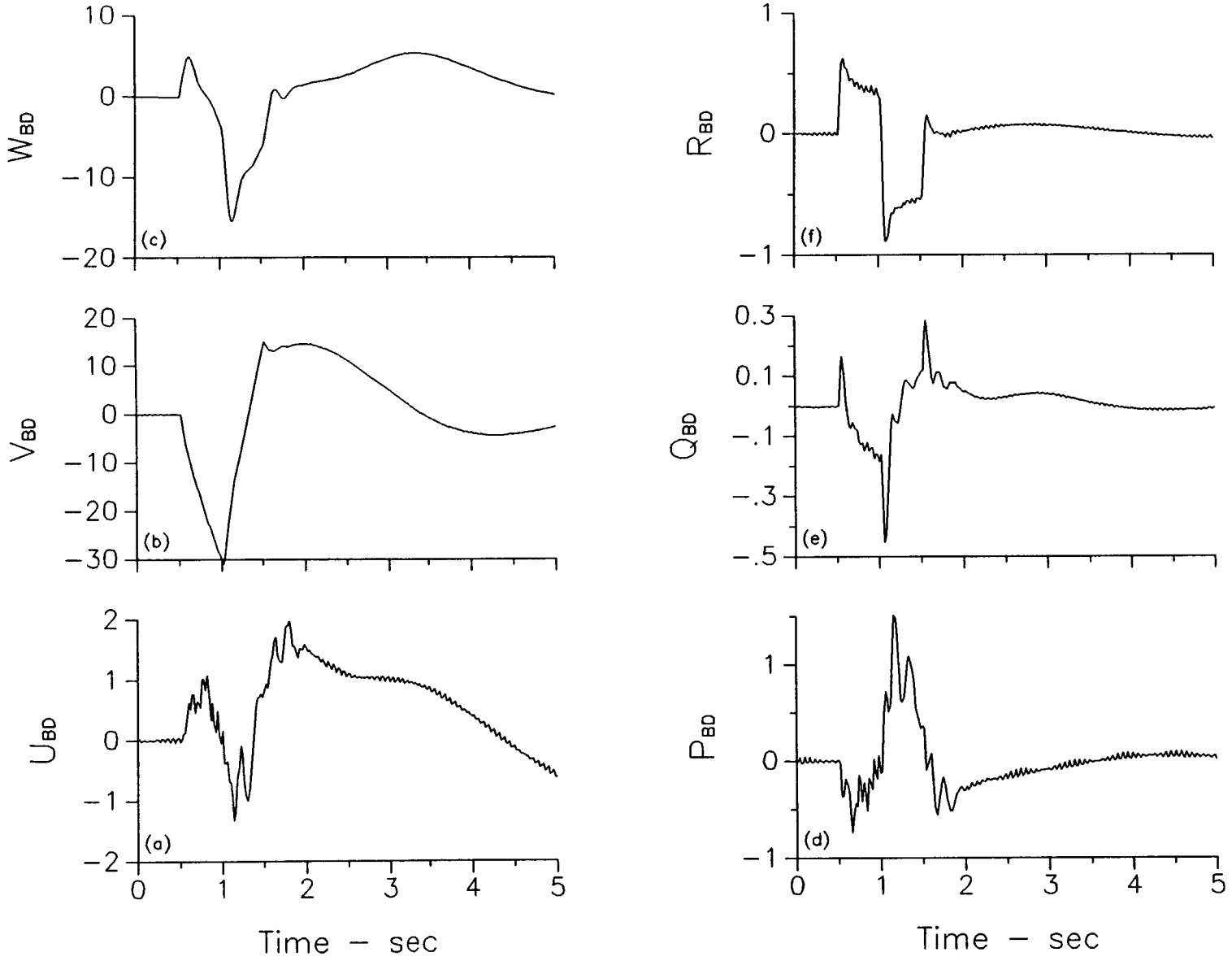

Figure 18.– Pedal (δ_p) dynamic check using subcycles.

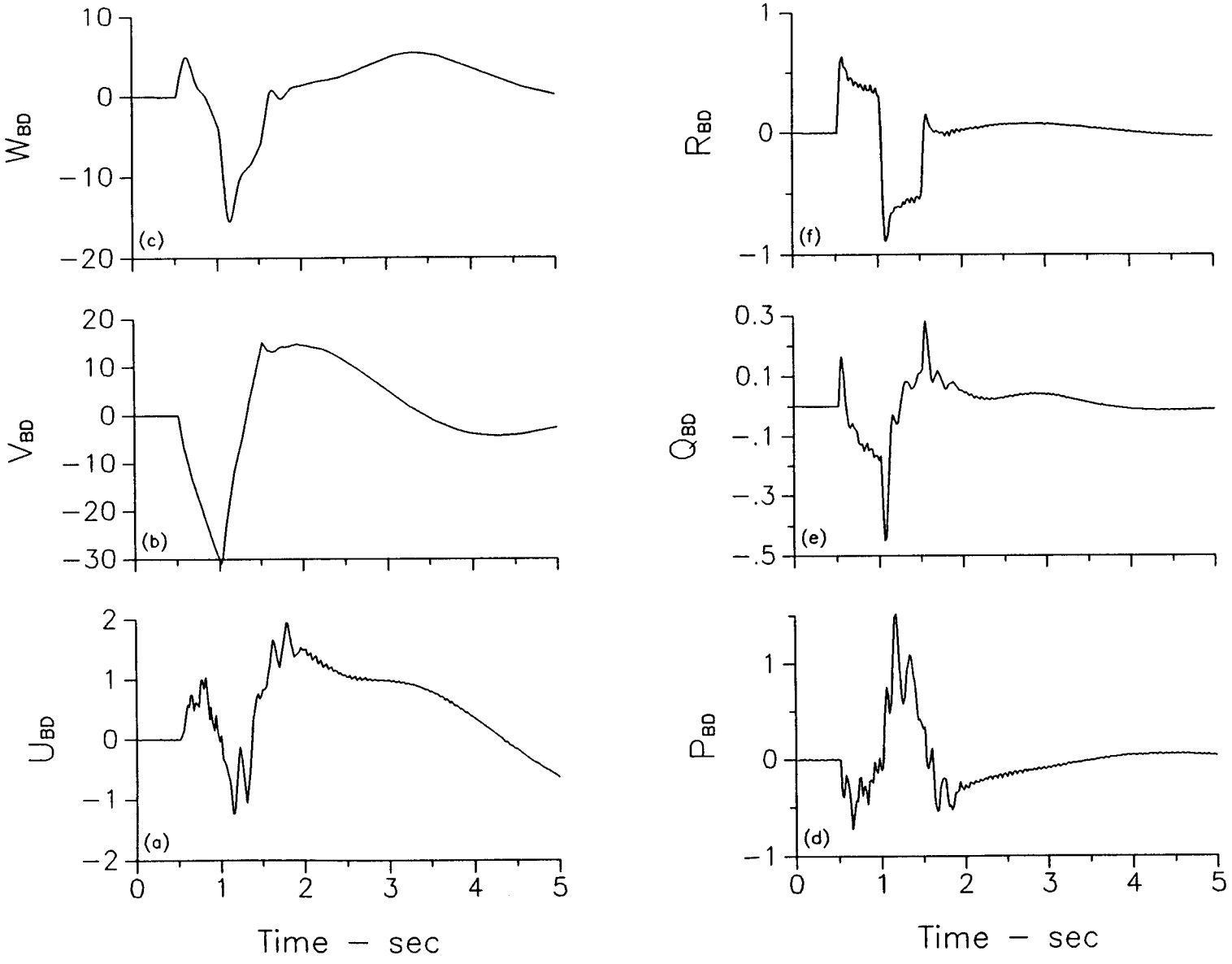

Figure 19.– Pedal (δ_p) dynamic check using subcycles and quiet mode.

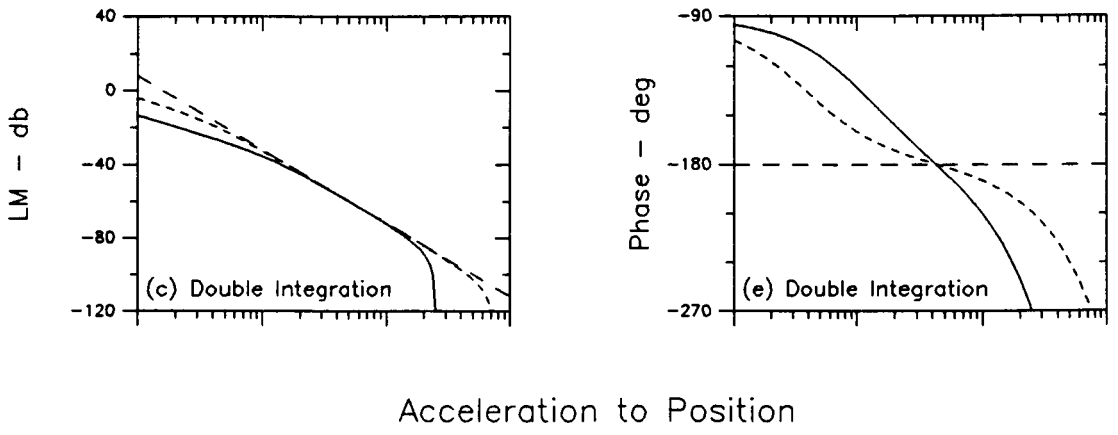

Figure 20.– Sikorsky integration algorithms.

NASA
National Aeronautics and Space Administration

Report Documentation Page

1. Report No.	2. Government Accession No.	3. Recipient's Catalog No.
NASA TM-102236		

4. Title and Subtitle	5. Report Date
Quiet Mode for Nonlinear Rotor Models	April 1990
	6. Performing Organization Code

7. Author(s)	8. Performing Organization Report No.
R. E. McFarland	A-89247
	10. Work Unit No. 505-66-29

9. Performing Organization Name and Address	11. Contract or Grant No.
Ames Research Center Moffett Field, CA 94035-1000	
	13. Type of Report and Period Covered Technical Memorandum
12. Sponsoring Agency Name and Address	
National Aeronautics and Space Administration Washington, DC 20546-0001	14. Sponsoring Agency Code

15. Supplementary Notes

Point of Contact: R. E. McFarland, Ames Research Center, MS 243-5
Moffett Field, CA 94035-1000
(415) 604-3863 or FTS 464-3863

16. Abstract

High frequency harmonics are generated by helicopter rotor systems, and nonlinear, blade-element models of these systems create the same harmonics. In discrete real-time rotorcraft simulation, however, especially for handling qualities research, they are more of a nuisance than a benefit. The cycle times required to adequately represent them are rarely obtainable. The result is that distinct frequencies alias into the pilot and simulator bandwidths, thereby decreasing simulation fidelity.

However, use of an interpolation procedure permits the observation of harmonics at their proper frequency locations, and an accompanying notch filter may then be used to attenuate the harmonics prior to decimation.

Rotorcraft simulations using these techniques are not contaminated with the spurious frequencies that create variable trim points, produce erroneous stability and control derivative data, and obscure time histories.

17. Key Words (Suggested by Author(s))	18. Distribution Statement
Notch filter, Aliasing, Simulation, Harmonics Interpolation, Rotorcraft, Decimation Attenuation, Blade element, Real-time Bandwidth, Discrete	Unclassified-Unlimited Subject Category – 5

19. Security Classif. (of this report)	20. Security Classif. (of this page)	21. No. of Pages	22. Price
Unclassified	Unclassified	38	A03